CD40 ligand induces RIP1-dependent, necroptosis-like cell death in low-grade serous but not serous borderline ovarian tumor cells

X Qiu[1], C Klausen[1], J-C Cheng[1] and PC K Leung*,[1]

Ovarian high-grade serous carcinomas (HGSCs) and invasive low-grade serous carcinomas (LGSCs) are considered to be distinct entities. In particular, LGSCs are thought to arise from non-invasive serous borderline ovarian tumors (SBOTs) and show poor responsiveness to conventional chemotherapy. The pro-apoptotic effects of CD40 ligand (CD40L) have been demonstrated in HGSC, though the underlying mechanisms are not fully understood. Conversely, the therapeutic potential of the CD40L-CD40 system has yet to be evaluated in LGSC. We now show that CD40 protein is focally expressed on tumor cells in two of five primary LGSCs compared with no expression in eight primary SBOTs. Treatment with CD40L or agonistic CD40 antibody decreased the viability of LGSC-derived MPSC1 and VOA1312 cells, but not SBOT3.1 cells. Small interfering RNA (siRNA) targeting CD40 was used to show that it is required for these reductions in cell viability. CD40L treatment increased cleaved caspase-3 levels in MPSC1 cells though, surprisingly, neither pan-caspase inhibitor nor caspase-3 siRNA reversed or even attenuated CD40L-induced cell death. In addition, CD40-induced cell death was not affected by knockdown of the mitochondrial proteins apoptosis-inducing factor (AIF) and endonuclease G (EndoG). Interestingly, CD40L-induced cell death was blocked by necrostatin-1, an inhibitor of receptor-interacting protein 1 (RIP1), and attenuated by inhibitors of RIP3 (GSK'872) or MLKL (mixed lineage kinase domain-like; necrosulfonamide). Our results indicate that the upregulation of CD40 may be relatively common in LGSC and that CD40 activation induces RIP1-dependent, necroptosis-like cell death in LGSC cells.
Cell Death and Disease (2015) **6,** e1864; doi:10.1038/cddis.2015.229; published online 27 August 2015

Epithelial ovarian cancer accounts for approximately 90% of all ovarian malignancies and is the leading cause of gynecological cancer death in developed countries.[1,2] Recently, differences in molecular alterations and clinico-pathological features have established a dualistic model dividing ovarian serous carcinomas into high-grade serous carcinoma (HGSC) and low-grade serous carcinoma (LGSC) subtypes. HGSCs are more common and are thought to develop directly from the ovarian surface epithelium or from serous tubal intra-epithelial carcinomas in the fallopian tube. In contrast, LGSCs are rare and are generally considered to develop from benign serous cystadenomas through serous borderline ovarian tumors (SBOT). SBOTs are slow-growing, non-invasive epithelial neoplasms that have a better prognosis compared with other types of ovarian cancer.[3–5] Our previous studies have shown that the inhibition of p53 or treatment of epidermal growth factor or transforming growth factor-β1 increases SBOT cell invasion by inducing epithelial–mesenchymal transition, which suggests a possible mechanism that mediates the progression from SBOT to LGSC.[6–9] However, many of SBOTs recur as LGSCs that display poor responsiveness to conventional chemotherapy and for which survival rates are < 50%.[1,3,10] Thus, the development of novel, targeted therapeutic strategies is likely required to significantly improve patient survival.

CD40, a transmembrane glycoprotein belonging to the tumor necrosis factor receptor superfamily, is expressed by a wide range of cell types including immune, endothelial and epithelial cells. Engagement of CD40 with its ligand, CD40L, has been shown to have important roles in a variety of physiological and pathological processes, especially in immunity.[11,12] In addition, CD40 expression has been demonstrated in several types of cancer, including colon, lung, cervical, bladder and prostate cancer.[13] However, reported functions of CD40 in tumor cells vary, with both pro-apoptotic and anti-proliferative effects observed depending on the cellular context.[14–16] Alternatively, some studies have shown that CD40 activation may promote the neoplastic transformation and growth of normal cells.[17–19] Expression of CD40 has been demonstrated in ovarian cancer cell lines and tumor samples, but not in normal ovarian tissue, suggesting that CD40 may have an important role in ovarian tumors.[20–24] Indeed, CD40L-CD40 signaling has been shown to induce growth-inhibitory effects in HGSC cells,[20,21,23–25] however, the therapeutic potential of CD40 in LGSC and SBOT has not been evaluated.

[1]Department of Obstetrics and Gynaecology, Child & Family Research Institute, University of British Columbia, Vancouver, British Columbia V5Z 4H4, Canada
*Corresponding author: PCK Leung, Department of Obstetrics and Gynaecology, Child & Family Research Institute, University of British Columbia, Room 317, 950 west 28th Avenue, Vancouver, British Columbia V5Z 4H4, Canada. Tel: +1 604 875 2718; Fax: +1 604 875 2717; E-mail: peter.leung@ubc.ca
Abbreviations: AIF, apoptosis-inducing factor; CD40L, CD40 ligand; EndoG, endonuclease G; HGSCs, high-grade serous carcinomas; LGSCs, low-grade serous carcinomas; 1-MT, 1-methyl-L-tryptophan; RIP1, receptor-interacting protein 1; RIP3, receptor-interacting protein 3; MLKL, mixed lineage kinase domain-like; RT-qPCR, reverse transcription quantitative real-time PCR; SBOTs, serous borderline ovarian tumors; siRNA, small interfering RNA

In the present study, we report for the first time elevated CD40 expression in a significant proportion of LGSCs compared with SBOTs. Moreover, CD40 expression is elevated in LGSC-derived MPSC1 and VOA1312 cells compared with SBOT3.1 cells, and CD40 activation induces cell death via CD40 only in LGSC-derived cells. Neither pan-caspase inhibitor nor caspase-3 small interfering RNA (siRNA) has any effect on CD40L-induced MPSC1 cell death. Moreover, CD40L-induced cell death was unaffected by individual or combined knockdown of the mitochondrial proteins apoptosis-inducing factor (AIF) and endonuclease G (EndoG). Interestingly, our results suggest that receptor-interacting protein 1 (RIP1), RIP3 and MLKL are involved in CD40-induced MPSC1 cell death. These results demonstrate that CD40 induces RIP1-dependent, necroptosis-like cell death in LGSC cells.

Results

Expression of CD40 in SBOT- and LGSC-derived cell lines and primary tumor samples. A previous study analyzing the DNA methylation profiles of ovarian serous neoplasms indicated that *CD40* is hypomethylated in LGSCs compared with SBOTs, suggesting the expression of CD40 may be higher in LGSCs than in SBOTs.[26] To test this hypothesis, we examined CD40 expression levels in SBOT-derived SBOT3.1 cells and LGSC-derived MPSC1 cells. CD40 mRNA (Figure 1a) and protein (Figure 1b) levels were higher in MPSC1 cells than in SBOT3.1 cells. As many CD40-expressing cells also express CD40L, we also examined the expression of CD40L in these two cell lines. As shown in Figure 1c, CD40L mRNA was undetectable in both SBOT3.1 and MPSC1 cells. These results suggest that both SBOT3.1 and MPSC1 cells express CD40, but that CD40 levels are much higher in LGSC-derived MPSC1 cells.

Next, we used western blot to measure CD40 protein levels in frozen tissues from eight SBOTs and five LGSCs. As shown in Figure 1d, CD40 protein levels were elevated in three of five LGSC samples compared with weak or no expression in the SBOT samples. To confirm CD40 expression in LGSC tumor cells, we immunostained matching sections from all eight SBOTs and five LGSCs. Focal, positive staining for CD40 was observed in tumor cells from two of five LGSC samples (Figures 1e and f). Interestingly, one of the LGSC samples with CD40-negative tumor cells contained multiple CD40-positive lymphoid follicles (Figure 1g), which are likely the cause of its positivity in western blot. Unlike the LGSC samples, all SBOT samples were negative for CD40 (Figure 1h).

CD40 activation induces cell death in LGSC-derived cells but not SBOT3.1 cells. Growth-inhibitory and pro-apoptotic effects of CD40 activation have previously been demonstrated in HGSC cells,[20,21,23-25] however, its effects on SBOT and LGSC cells are unknown. To investigate the effects of CD40L on SBOT and LGSC, SBOT3.1 and MPSC1 cells were treated for 48 h with 500 ng/ml recombinant human CD40L and morphology was assessed by phase contrast microscopy. As shown in Figure 2a, treatment with CD40L did not affect the morphology of SBOT3.1 cells; however, it

significantly decreased the number of MPSC1 cells, suggesting potential pro-apoptotic effects of CD40L in MPSC1 cells. To expand on these findings, MPSC1 and SBOT3.1 cells were treated for 24, 48 or 72 h with different concentrations of CD40L (20, 100 or 500 ng/ml) and cell viability was examined by the MTT assay (Figures 2b and c). CD40L treatment did not diminish SBOT3.1 cell viability, but it reduced that of MPSC1 cells in both a time- and concentration- dependent manner, with the most significant reductions occurring 72 h after treatment. To further confirm these effects on cell viability, we measured viable cell numbers by Trypan blue exclusion assay following treatment with 500 ng/ml CD40L for 24, 48 or 72 h. In agreement with our MTT results, CD40L treatment induced time-dependent reductions in viable MPSC1 cell numbers but did not alter SBOT3.1 cell viability (Figures 2d and e). Moreover for both methods, the number of viable cells at 72 h was significantly lower than that at 24 or 48 h, indicating that CD40L-induced decreases in MPSC1 cell viability are mediated, at least in part, by increased cell death. Interestingly, we do not believe that low CD40 levels are entirely responsible for the lack of response in SBOT3.1 cells, because these cells can produce CD40L-induced increases in ERK1/2 phosphorylation that are comparable with those observed in MPSC1 cells (Supplementary Figure 1).

Next, we examined the effects of CD40 ligation on MPSC1 cell viability by treating the cells with agonistic CD40 antibody. As shown in Figures 2f and g, similar reductions in MPSC1 cell viability or viable cell numbers were observed following treatment for 72 h with 500 ng/ml agonistic CD40 antibody. To further confirm that CD40 activation reduces the viability of LGSC cells, we examined the effects of CD40L on LGSC-derived VOA1312 cells[27] which have CD40 protein levels similar to those of MPSC1 cells (Figure 2h). As shown in Figure 2i, VOA1312 cell viability was reduced following treatment for 72 h with 500 ng/ml CD40L. To determine whether CD40 is required for CD40L-induced cell death in LGSC cells, we examined the effects of CD40L on cell viability following siRNA-mediated knockdown of endogenous CD40. Pre-treatment of MPSC1 cells for 24 h with CD40 siRNA significantly reduced CD40 protein levels (Figure 3a), and reversed the effects of subsequent treatment for 72 h with 500 ng/ml of either CD40L (Figures 3b and c) or agonistic CD40 antibody (Figures 3d and e) on cell viability as assessed by MTT or Trypan blue exclusion assays. In addition, knockdown of CD40 also reversed the effects of CD40L on cell viability in VOA1312 cells (Figure 3f).

Caspase-3 is activated during CD40L-induced MPSC1 cell death. Next, we sought to determine whether apoptosis, a well-known form of programmed cell death, was involved in CD40L-induced MPSC1 cell death. Cleavage and activation of caspase-3, a critical executioner caspase, is often associated with apoptotic cell death.[28,29] Thus, we used western blot to measure cleaved caspase-3 levels in MPSC1 cells following treatment for 24 or 48 h with CD40L (100 or 500 ng/ml). CD40L treatment increased the levels of cleaved caspase-3 after 48 h in MPSC1 cells (Figure 4a). Consistent with our cell viability results, treatment of SBOT3.1 cells for 48 h with CD40L (100 or 500 ng/ml) did
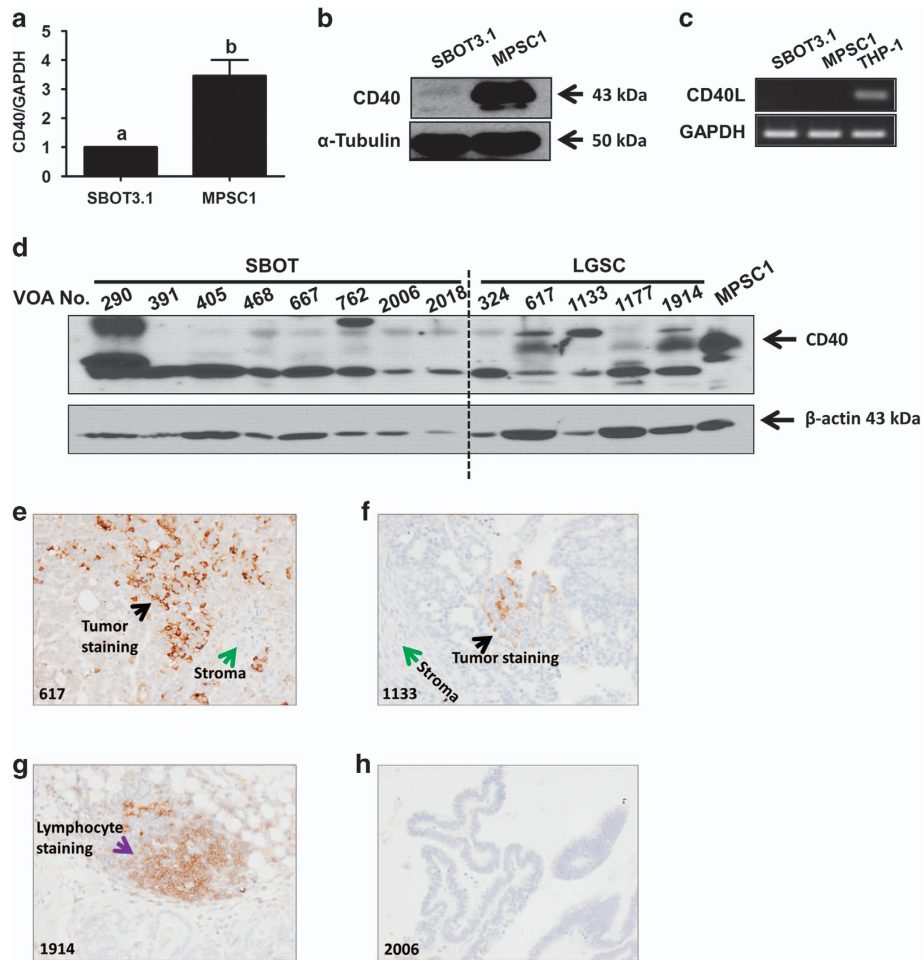
Figure 1 Expression of CD40 in SBOT- and LGSC-derived cell lines and primary tumor samples. (**a** and **b**) RT-qPCR and western blot were used to measure endogenous CD40 mRNA and protein levels in SBOT-derived SBOT3.1 cells and LGSC-derived MPSC1 cells. Quantitative results are expressed as the mean ± S.E.M. of at least three independent passages and values without a common letter are significantly different (*P* < 0.05). (**c**) Endogenous CD40L mRNA levels in SBOT3.1 and MPSC1 cells were measured by RT-qPCR. THP-1 human acute monocytic leukemia cells were used as a positive control and RT-qPCR products were analyzed by agarose gel electrophoresis. (**d**) Western blot was used to measure endogenous CD40 protein levels in MPSC1 cells (positive control) and frozen tissues from primary SBOTs and LGSCs (labeled with 'VOA#'). (**e**–**h**) Representative CD40 immunostaining results for matched sections from the patient samples analyzed by western blot

not alter the levels of cleaved caspase-3 (Figure 4b). Importantly, CD40L-induced increases in cleaved caspase-3 levels were abolished by pre-treatment of MPSC1 cells for 24 h with CD40 siRNA (Figure 4c). These results indicate that CD40L/CD40 signaling can activate caspase-3 in LGSC-derived MPSC1 cells but not SBOT3.1 cells.

CD40L-induced MPSC1 cell death is caspase-independent. To determine whether activated caspase-3 is directly involved in CD40L-induced cell death, MPSC1 cell viability and cleaved caspase-3 levels were examined in the presence or absence of an irreversible pan-caspase inhibitor (Boc-D-FMK). Pre-treatment for 2 h with 20 μM Boc-D-FMK completely blocked CD40L-induced increases in cleaved caspase-3 levels (Figure 5a). Surprisingly, pre-treatment with Boc-D-FMK (20, 50 or 100 μM) did not reverse, or even attenuate, the effects of CD40L (500 ng/ml, 72 h) on cell viability as measured by MTT assay (Figure 5b). To confirm these findings, we examined the effects of CD40L on MPSC1 cell viability following siRNA-mediated knockdown of

caspase-3. Pre-treatment for 24 h with caspase-3 siRNA significantly reduced pro-caspase-3 protein levels (Figure 5c), but did not alter the effects of subsequent treatment with CD40L (500 ng/ml, 72 h) on cell viability as measured by MTT or Trypan blue exclusion assays (Figures 5d and e). These results suggest that CD40L-induced cell death in LGSC-derived MPSC1 cells is caspase-independent.

CD40L induces RIP1-dependent, necroptosis-like cell death in MPSC1 cells. Mitochondria are central to the control of cell death, and mitochondria-dependent cell death is characterized by the release of mitochondrial proteins into the cytoplasm that are capable of inducing caspase-dependent or caspase-independent cell death.[30,31] AIF and EndoG are mitochondrial proteins that are known to translocate to the nucleus and cause chromatin condensation and DNA cleavage in a caspase-independent manner.[32,33] To determine whether AIF and/or EndoG are required for CD40L-induced MPSC1 cell death, we examined the effects
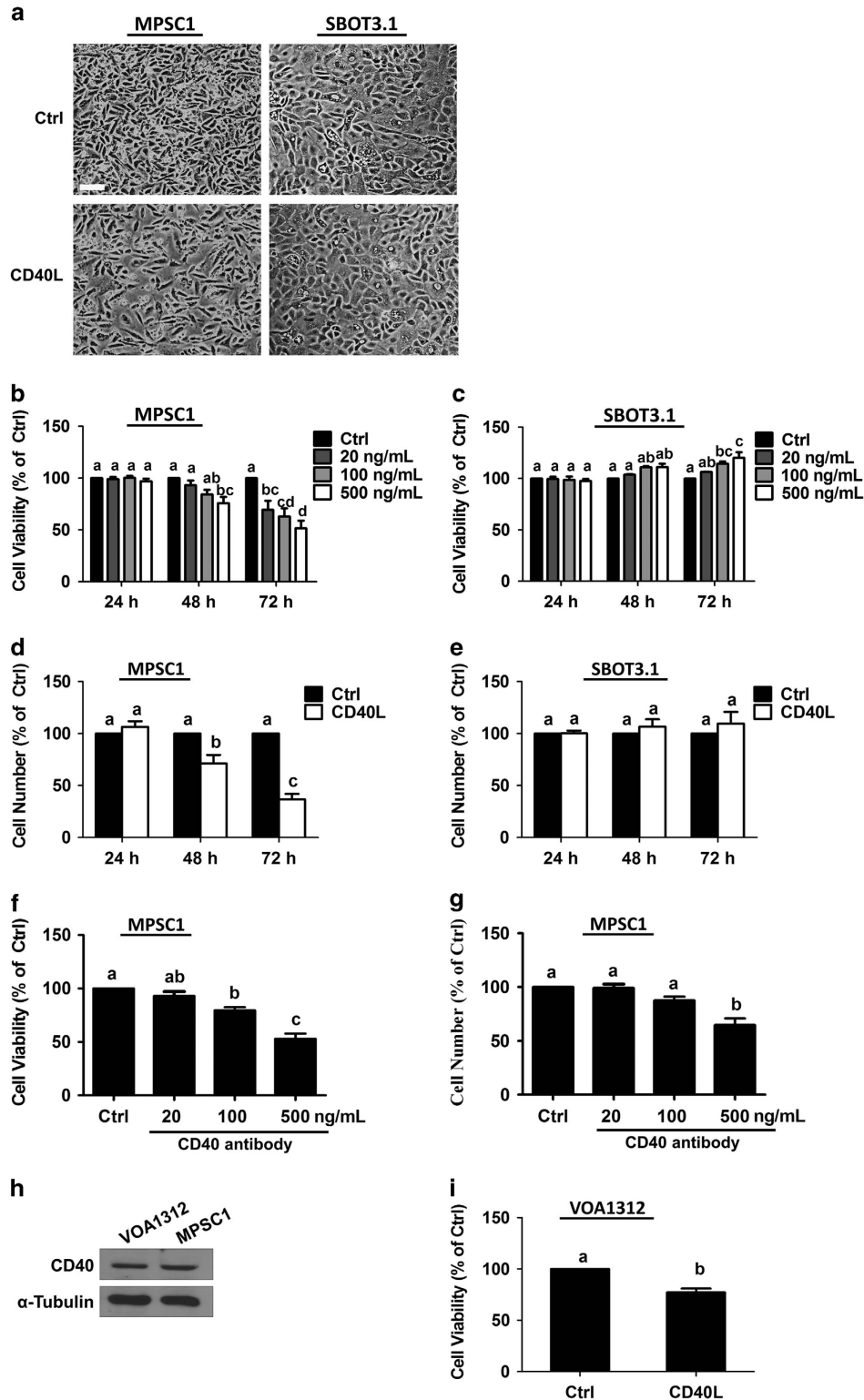
Figure 2 CD40 activation induces cell death in MPSC1 not SBOT3.1 cells. (**a**) Cells were treated for 48 h with vehicle control (Ctrl) or 500 ng/ml recombinant human CD40L, and cell morphology was assessed by phase contrast microscopy. Scale bar: 200 μM. (**b** and **c**) Cells were treated for 24, 48 or 72 h with vehicle control (Ctrl) or different concentrations of CD40L and cell viability was examined by the MTT assay. (**d** and **e**) Alternatively, viable cell numbers were measured by Trypan blue exclusion assay following treatment for 24, 48 or 72 h with vehicle control or 500 ng/ml CD40L. (**f** and **g**) Cells were treated for 72 h with vehicle control or different concentrations of agonistic CD40 antibody and cell viability (**f**) and cell number (**g**) were analyzed by MTT and Trypan blue exclusion assays, respectively. (**h**) Western blot was used to measure endogenous CD40 protein levels in VOA1312 and MPSC1 cells. (**i**) VOA1312 cells were treated for 72 h with vehicle control or 500 ng/ml CD40L and cell viability was examined by the MTT assay. Results are expressed as the mean ± S.E.M. of at least three independent experiments. Values without a common letter are significantly different ($P < 0.05$)
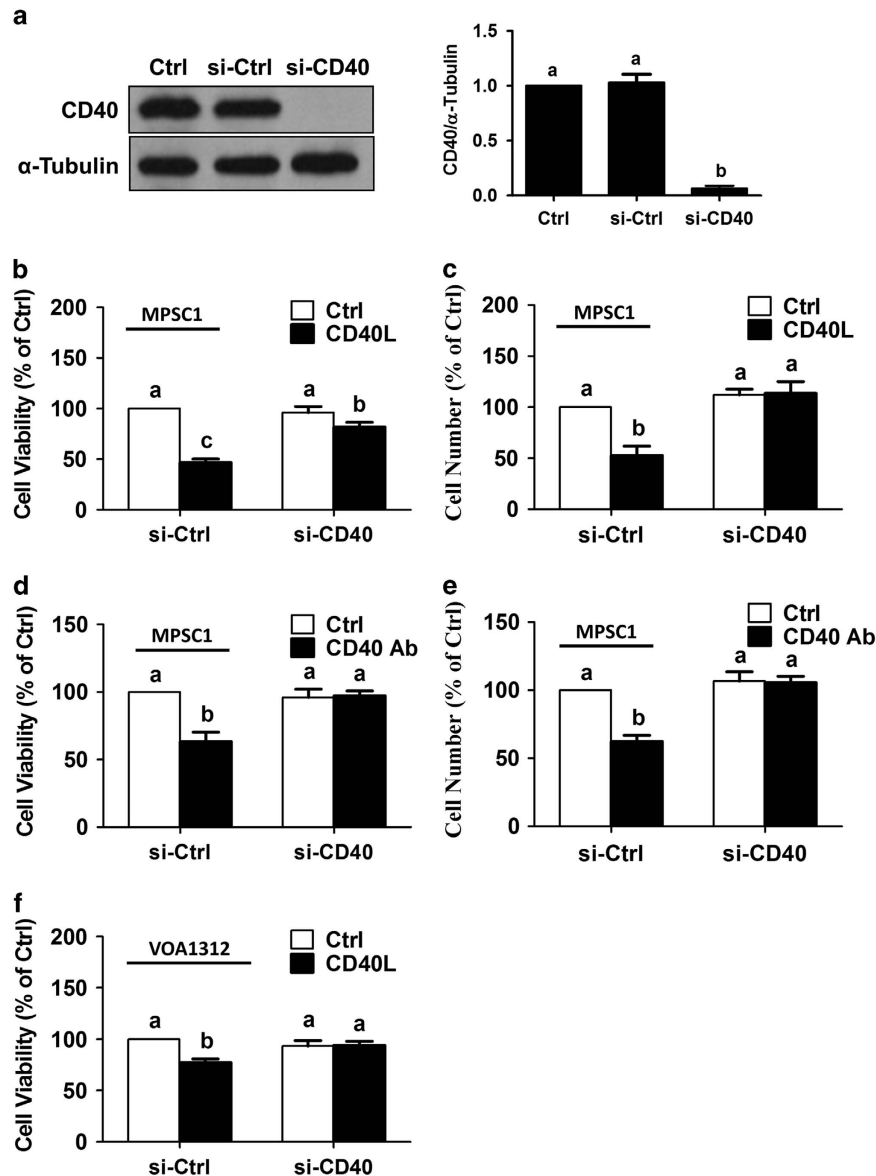
Figure 3 CD40 is required for CD40L-induced cell death. (**a**) MPSC1 cells were transfected for 24 h with 50 nM control siRNA (si-Ctrl) or CD40 siRNA (si-CD40) and knockdown efficiency was examined by western blot. Following transfection as described in (**a**), MPSC1 cells were treated for 72 h with vehicle control (Ctrl) or 500 ng/ml CD40L (**b** and **c**) or agonistic CD40 antibody (**d** and **e**) and cell viability (**b** and **d**) and cell number (**c** and **e**) were analyzed by MTT and Trypan blue exclusion assays, respectively. (**f**) VOA1312 cells were transfected for 24 h with 50 nM control siRNA or CD40 siRNA, treated for another 72 h with vehicle control or CD40L (500 ng/ml), and cell viability was examined by the MTT assay. Results are expressed as the mean ± S.E.M. of at least three independent experiments. Values without a common letter are significantly different ($P < 0.05$)

of CD40L on cell viability following siRNA-mediated knockdown of endogenous AIF and/or EndoG. Pre-treatment for 24 h with AIF and/or EndoG siRNA significantly reduced AIF and EndoG mRNA levels (Figure 6a), but did not alter the effects of subsequent treatment with CD40L (500 ng/ml, 72 h) on cell viability as measured by MTT assay (Figure 6b). These results suggest that CD40L-induced cell death in LGSC-derived MPSC1 cells is mitochondria-independent.

RIP1 and RIP3 kinases have emerged as important regulators of a form of caspase-independent cell death referred to as necroptosis.[34,35] To determine whether RIP1 is required for CD40L-induced cell death, MPSC1 cell viability was measured in the presence or absence of an allosteric

inhibitor of RIP1 (necrostatin-1). Interestingly, pre-treatment for 2 h with 150 nM necrostatin-1 completely blocked CD40L-induced reductions in cell viability as measured by MTT assay (Figure 6c). However, several studies have shown that necrostatin-1 also inhibits indoleamine-2,3-dioxygenase.[36,37] To exclude the possible involvement of indoleamine-2,3-dioxygenase, MPSC1 cells were pre-treated for 2 h with the indoleamine-2,3-dioxygenase inhibitor 1-methyl-L-tryptophan (1-MT, 150 nM) prior to being treated for 72 h with 500 ng/ml CD40L. As shown in Figure 6d, CD40L-induced reductions in cell viability were not affected by treatment with 1-MT. To further confirm the involvement of RIP1 in CD40L-induced cell death, we examined the effects of CD40L on cell viability
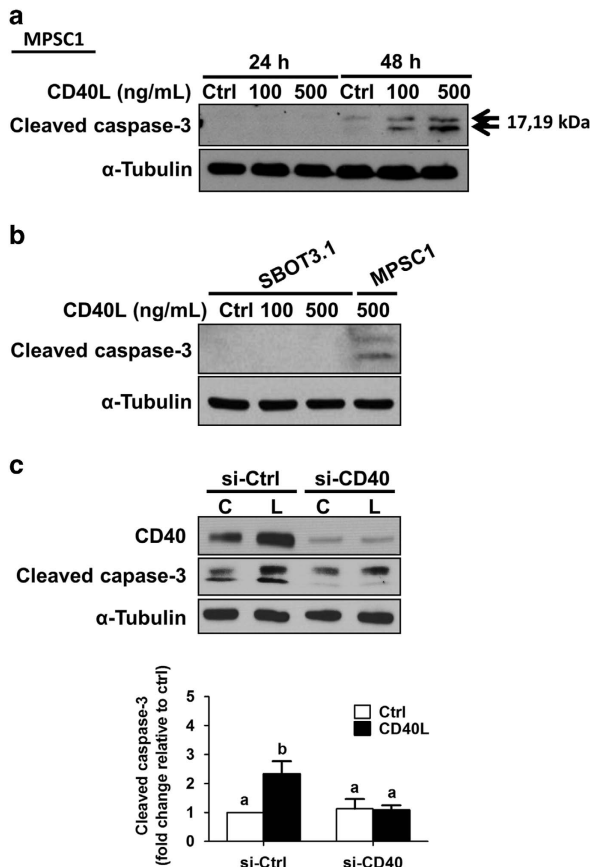
a

b

c

Figure 4 Caspase-3 is activated during CD40L-induced MPSC1 cell death. (**a**) Cleaved caspase-3 levels were measured by western blot following treatment of MPSC1 cells for 24 or 48 h with vehicle control (Ctrl) or CD40L (100 or 500 ng/ml). (**b**) SBOT3.1 cells were treated for 48 h with vehicle control (Ctrl) or CD40L and cleaved caspase-3 levels were measured by western blot. (**c**) MPSC1 cells were transfected for 24 h with 50 nM control siRNA (si-Ctrl) or CD40 siRNA (si-CD40) and then treated for another 48 h with vehicle control (Ctrl) or CD40L (500 ng/ml). CD40 and cleaved caspase-3 were analyzed by western blot and quantified cleaved caspase-3 levels (right) are expressed as the mean ± S.E.M. of at least three independent experiments. Values without a common letter are significantly different ($P < 0.05$)

following siRNA-mediated knockdown of endogenous RIP1. Pre-treatment for 24 h with RIP1 siRNA significantly reduced RIP1 protein levels (Figure 6e), and partially reversed the effects of subsequent treatment with CD40L (500 ng/ml, 72 h) on cell viability as assessed by MTT or Trypan blue exclusion assays (Figures 6f and g). Increasing evidence suggests that interactions between RIP1 and RIP3 are crucial to necrosome formation, and that MLKL (mixed lineage kinase domain-like), a critical substrate of RIP3, is a key effector of necroptosis.[35,38] To investigate the involvement of RIP3 and MLKL in CD40-induced cell death, MPSC1 cell viability was measured in the presence or absence of specific inhibitors of RIP3 (GSK'872) or MLKL (necrosulfonamide). As shown in Figure 6h, pre-treatment for 2 h with GSK'872 or necrosulfonamide partially reversed CD40L-induced reductions in cell viability as measured by MTT assay. Collectively, these data suggest that CD40 induces RIP1-dependent, necroptosis-like cell death in MPSC1 cells.

Discussion

Invasive LGSCs display poor responsiveness to conventional chemotherapy, thus novel therapeutic strategies are urgently required to improve patient survival. We now show that CD40 protein is expressed in a significant proportion of LGSCs, perhaps as many as half, compared with weak or no expression in SBOTs. These results are consistent with a previous study suggesting hypomethylation of *CD40* in LGSCs compared with SBOTs,[26] though future studies will be required to confirm an epigenetic basis for elevated CD40 expression in LGSCs. Importantly, we show for the first time that treatment with CD40L or agonistic CD40 antibody induces cell death in LGSC-derived cells via CD40 activation. Thus, recombinant human CD40L or agonistic CD40 antibody could represent novel treatment options for patients with LGSC displaying elevated CD40. Anti-tumor effects for CD40L-CD40 signaling have been shown in various types of CD40-positive tumors, with direct apoptotic cell killing accounting for much of the response.[39–43] Indeed, recombinant CD40L treatment of CD40-positive HGSC xenografts in severe combined immunodeficient mice induced significant apoptosis and tumor destruction, and increased the efficacy of suboptimal doses of cisplatin.[25]

In addition to directly inducing tumor cell death, CD40-targeted treatments can stimulate general immune activation and have demonstrated utility as cancer immunotherapies, for which CD40 expression on tumor cells is not necessary.[44] Activation of CD40 on antigen-presenting cells licenses them to stimulate T-killer cells to exert killing responses.[45] Several studies have demonstrated the effectiveness of CD40 ligation in triggering the elimination of tumor cells by T-killer cells.[46,47] Moreover, CD40-induced anti-tumor effects have also been shown to involve activated macrophages[48,49] as well as B cells and natural killer cells.[50–52] Interestingly, our immunostaining results show that some primary LGSCs with CD40-negative tumor cells contain CD40-positive lymphoid cells. In this context, patients with SBOT or LGSC displaying weak or no expression of CD40 may still benefit from CD40-targeted therapies owing to the enhancement of antigen-presenting cell function and the activation of T cells and natural killer cells. Patients with CD40-positive LGSC could also benefit from enhanced immune activation, including opsonization effects if treated with anti-CD40 antibody. Future studies investigating the potential of CD40-targeted therapies on CD40-positive and -negative LGSCs *in vivo* will be of great interest.

Cell death can occur in several ways including necrosis, apoptosis and necroptosis. Apoptosis, a form of programmed cell death, is accompanied by a host of morphological and biochemical features, including plasma membrane blebbing, cell shrinkage, chromatin condensation, apoptotic bodies, DNA fragmentation and phosphatidylserine exposure.[53,54] Caspases are the primary effectors of apoptotic cell death and caspase-3 is considered an important executioner owing to its activation of the endonuclease CAD, which can degrade chromosomal DNA.[55] Interestingly, though treatment with CD40L resulted in caspase-3 activation, it was not required for CD40L-induced MPSC1 cell death. Moreover, redundant effects from other caspases are unlikely because CD40L-induced cell death was unaffected by pre-treatment with the
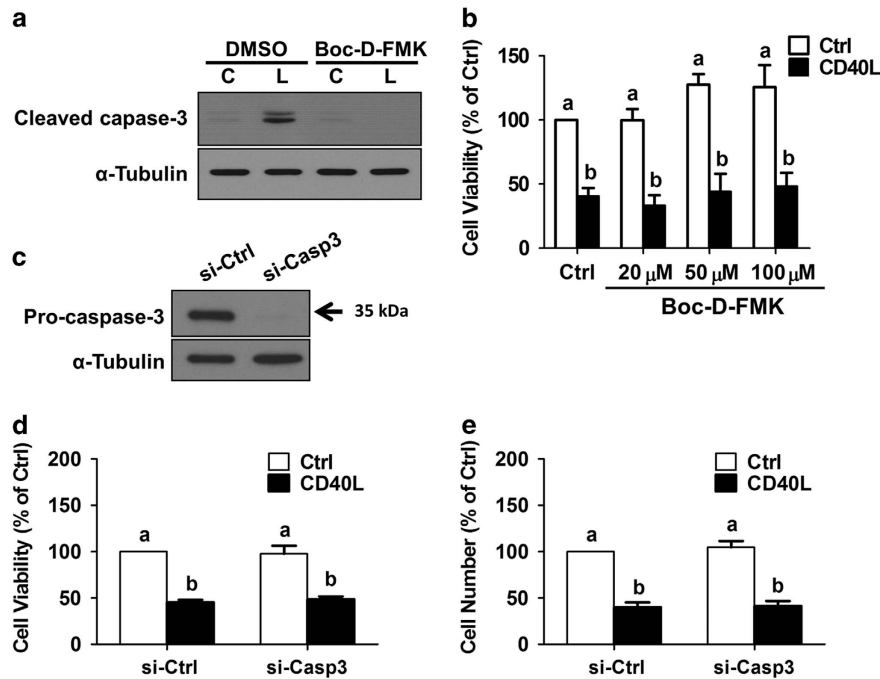
Figure 5 CD40L-induced MPSC1 cell death is caspase-independent. (**a**) Cells were pre-treated for 2 h with or without 20 μM Boc-D-FMK and then treated for 48 h with vehicle control (Ctrl) or CD40L (500 ng/ml). Cleaved caspase-3 levels were measured by western blot. (**b**) Cell viability was measured by MTT assay following treatment for 72 h with vehicle control or CD40L (500 ng/ml) in the presence or absence of different concentrations of Boc-D-FMK (20, 50 or 100 μM). (**c**) Cells were transfected for 24 h with 50 nM control siRNA (si-Ctrl) or caspase-3 siRNA (si-Casp3) and knockdown efficiency was examined by western blot. Following transfection as described in (**c**), cells were treated for 72 h with vehicle control or CD40L (500 ng/ml) and cell viability (**d**) and cell number (**e**) were analyzed by MTT and Trypan blue exclusion assays, respectively. Results are expressed as the mean ± S.E.M. of at least three independent experiments. Values without a common letter are significantly different ($P < 0.05$)

broad-spectrum caspase inhibitor Boc-D-FMK. Interestingly, beyond their critical roles in apoptosis, increasing evidence suggests a variety of non-apoptotic functions of caspases.[56,57] For example, caspase-3 is transiently activated and functions as a key protease in the processes of erythroid differentiation[58] and maturation.[59] Caspase-3 has also been shown to inhibit B-cell cycling,[60] promote adult hematopoietic stem cell quiescence[61] and mediate embryonic stem cell differentiation.[62] Thus, CD40L-induced caspase-3 activation in LGSC cells could indicate additional non-apoptotic roles that warrant further investigation.

Caspase-independent forms of cell death have also been described, often involving the release of mitochondrial proteins such as AIF and EndoG.[30,31,63] Upon release, AIF and EndoG translocate to the nucleus where they induce DNA fragmentation and chromosome condensation.[32,33,63] Though caspase-independent, CD40L-induced MPSC1 cell death does not appear to involve AIF and/or EndoG. Rather, our RIP1 inhibitor (necrostatin-1) and siRNA findings suggest that CD40L induces necroptosis, a form of controlled necrosis characterized by a dependency on RIP1, RIP3 and MLKL when caspases, especially caspase-8, are inhibited.[34,35,64–66] Indeed, the induction of necroptosis-like cell death by CD40 activation is further supported by our RIP3 (GSK'872) and MLKL (necrosulfonamide) inhibitor results. RIP1-mediated necroptosis is becoming increasingly recognized as an important form of caspase-independent cell death,[34,67] however, pro-apoptotic roles for RIP1 have also been described in caspase-dependent, death receptor-mediated cell killing.[68,69] In EJ bladder cancer cells, RIP1 has been shown to mediate

CD40L-induced caspase-8 activation and apoptosis, the latter being partially inhibited by necrostatin-1 and completely abolished by pan-caspase inhibitor.[70] Moreover, the relationship of RIP1 to necroptosis can also vary depending on the cellular context, as recent studies have demonstrated that RIP1 may inhibit rather than promote necroptosis.[71] This variation likely reflects the complex regulatory roles and interactions of RIP1 with other proteins involved in necrosome formation and necroptotic cell death. Indeed, such variation could explain the discrepancy between our RIP1 inhibitor and siRNA results such that RIP1 still acts as a crucial scaffold for protein–protein interactions when cells are treated with inhibitor (necrostatin-1), whereas this scaffold function would be disrupted when treating cells with siRNA.[35,72] Future research will be required to characterize, in detail, the precise molecular determinants of CD40L-induced cell death in LGSCs.

In summary, we have shown that CD40 is upregulated in a significant proportion of LGSCs (including LGSC-derived MPSC1 and VOA1312 cells) compared with SBOTs. CD40 activation induces RIP1-dependent, necroptosis-like cell death in MPSC1 but not SBOT3.1 cells. These findings provide insight into the function and therapeutic potential of the CD40 system in LGSCs.

Materials and Methods
Cell culture. The SBOT3.1,[73,74] MPSC1[75] and VOA1312[27] cell lines were kindly provided by Dr. Nelly Auersperg (Department of Obstetrics and Gynaecology, University of British Columbia, Canada), Dr Ie-Ming Shih (Department of Pathology, Johns Hopkins Medical Institutions, USA) and Dr David G. Huntsman (Department
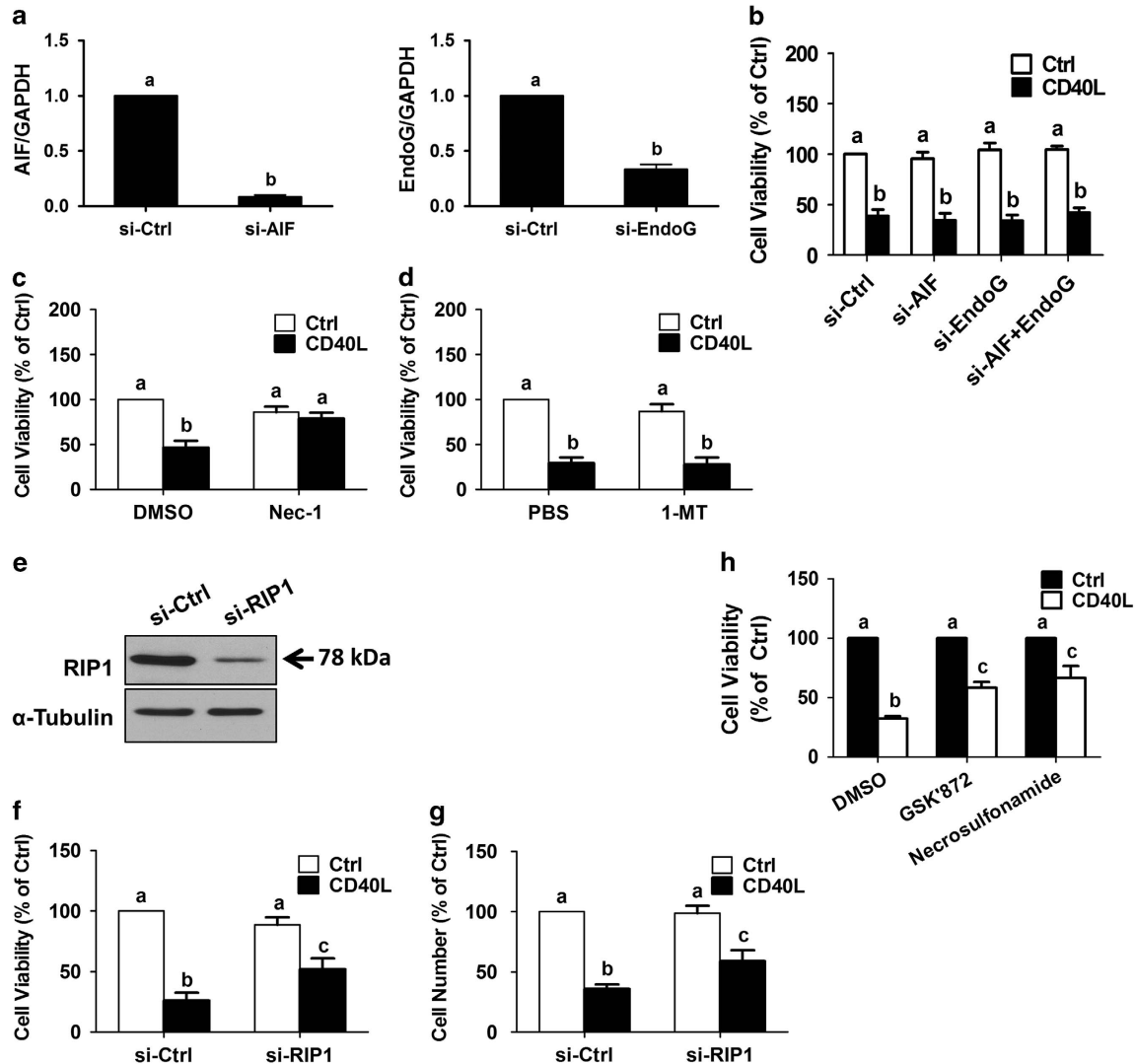
Figure 6 CD40L induces mitochondria-independent but RIP1-dependent cell death in MPSC1 cells. (**a**) Cells were transfected for 24 h with 50 nM control siRNA (si-Ctrl), AIF siRNA (si-AIF) or EndoG siRNA (si-EndoG), and knockdown efficiency was examined by RT-qPCR. (**b**) Cells were transfected for 24 h with the indicated siRNAs alone or in combination prior to being treated for 72 h with vehicle control (Ctrl) or CD40L (500 ng/ml). Cell viability was measured by MTT assay. (**c** and **d**) Cell viability was measured by MTT assay following treatment for 72 h with vehicle control or CD40L (500 ng/ml) in the presence or absence of 150 nM necrostatin-1 (**c**) or 1-MT (D). (**e**) Cells were transfected for 24 h with 50 nM control siRNA or RIP1 siRNA (si-RIP1), and knockdown efficiency was examined by western blot. Following transfection as described in (**e**), transfected cells were treated for 72 h with vehicle control or CD40L (500 ng/ml), and cell viability (**f**) and cell number (**g**) were analyzed by MTT and Trypan blue exclusion assays, respectively. (**h**) Cell viability was measured by MTT assay following treatment for 72 h with vehicle control or CD40L (500 ng/ml) in the presence or absence of 6 μM GSK'872 or 3 μM necrosulfonamide. Results are expressed as the mean $\pm$ S.E.M. from at least three independent experiments. Values without a common letter are significantly different ($P < 0.05$)

of Pathology and Laboratory Medicine, University of British Columbia, Canada), respectively. SBOT3.1 and VOA1312 cells were grown in a 1 : 1 (v/v) mixture of M199/MCDB105 medium (Sigma-Aldrich, Oakville, ON, Canada) supplemented with 10% fetal bovine serum (Hyclone Laboratories Inc., Logan, UT, USA). MPSC1 cells were maintained in RPMI 1640 medium (Invitrogen, Burlington, ON, Canada) supplemented with 10% fetal bovine serum. Cells were cultured at 37 °C in a humidified atmosphere containing 5% CO_2 and 95% air.

Frozen tissue samples. Frozen samples of primary tissue were obtained from the Ovarian Cancer Canada Tumor Bank with informed patient consent following approval from the University of British Columbia and British Columbia Cancer Agency Research Ethics Board. A cube of tissue was quickly removed from the cryovial, minced using a scalpel blade and transferred to a tube containing cell lysis buffer (Cell Signaling Technology, Danvers, MA, USA) with protease inhibitor cocktail (Sigma-Aldrich). Lysates were passed at least five times each through 18- and 22-gauge needles. Extracts were centrifuged at 20 000 × g for 10 min at 4 °C

to remove cellular debris and supernatants were transferred to a clean microcentrifuge tube. Samples were stored at −80 °C until assayed by western blot as described below.

Antibodies and reagents. Mouse monoclonal anti-α-Tubulin, goat polyclonal anti-actin (C-11) and rabbit polyclonal anti-CD40 (N-16) antibodies were obtained from Santa Cruz Biotechnology (Santa Cruz, CA, USA). Polyclonal anti-caspase-3 and anti-RIP1 antibodies were obtained from Cell Signaling Technology. Mouse monoclonal agonistic anti-CD40 (Clone # 82111) antibody was purchased from R&D Systems (Minneapolis, MN, USA). Horseradish peroxidase-conjugated goat anti-mouse IgG and goat anti-rabbit IgG were obtained from Bio-Rad Laboratories (Hercules, CA, USA). Recombinant human sCD40 ligand (CD40L) was obtained from Peprotech (Rocky Hill, NJ, USA). 3-(4,5-Dimethylthiazol-2-yl)-2,5-diphenylte-trazolium bromide (MTT), necrostatin-1 and 1-MT were purchased from Sigma-Aldrich. Boc-D-FMK was purchased from Abcam (Toronto, ON, Canada). GSK'872 and necrosulfonamide were purchased from Millipore (Etobicoke, ON, Canada).

SiRNA transfection. To knockdown endogenous CD40, caspase-3, AIF, EndoG or RIP1, cells were transfected with 50 nM ON-TARGET*plus* SMARTpool siRNA or ON-TARGET*plus* Non-targeting Control Pool (Dharmacon, Lafayette, CO, USA) using Lipofectamine RNAiMAX (Invitrogen, Burlington, ON, USA).

Western blot analysis. Cells were washed with cold PBS and lysed in lysis buffer (Cell Signaling Technology) containing protease inhibitor cocktail (Sigma-Aldrich). Extracts were centrifuged at $20\,000 \times g$ for 10 min at 4 °C and protein concentrations were determined using the DC Protein Assay (Bio-Rad Laboratories) with BSA as the standard. Equal amounts of protein were separated by SDS-polyacrylamide gel electrophoresis and transferred to polyvinylidene fluoride membranes. After blocking with Tris-buffered saline containing 5% non-fat dry milk for 1 h, the membranes were incubated overnight at 4 °C with primary antibodies followed by incubation with peroxidase-conjugated secondary antibody. Immunoreactive bands were detected using enhanced chemiluminescent substrate (Pierce, Rockford, IL, USA) followed by exposure to CL-XPosure film (Thermo Fisher, Waltham, MA, USA). Films were scanned and quantified by densitometry using Scion image software (Scion Corp., Frederick, MD, USA). CD40 and cleaved caspase-3 levels were normalized to α-tubulin. Alternatively, CD40 levels in primary tumor samples were normalized to actin.

Immunohistochemistry. Formalin-fixed, paraffin-embedded tumor samples were assessed for CD40 expression. Sections were deparaffinized in xylene, rehydrated through graded alcohol, and processed for wet heat-induced antigen retrieval in a steamer for 20 min with a modified citrate buffer (pH 6.1; Dako, Burlington, ON, Canada). Endogenous peroxidase activity was quenched with 3% hydrogen peroxide in PBS for 30 min. Sections were blocked with serum-free protein block (Dako) for 30 min at room temperature, and then incubated overnight at 4 °C with polyclonal anti-CD40 (Abcam, Ab13545) diluted 1 : 250 in a serum-free protein block. Immunoreactivity was detected with the LSAB+HRP System (Dako) and 3,3′-diaminobenzidine chromogen solution (Dako). Slides were counterstained with hematoxylin (Sigma), dehydrated through graded alcohol to xylene, mounted with xylene-based mounting medium and evaluated by light microscopy.

Reverse transcription quantitative real-time PCR (RT-qPCR). Total RNA was extracted using TRIzol Reagent (Invitrogen) according to the manufacturer's instructions. Reverse transcription was performed with $3\,\mu$g RNA, random primers and M-MLV reverse transcriptase (Promega, Madison, WI, USA). RT-qPCR was performed using an Applied Biosystems (Burlington, ON, Canada) 7300 Real-Time PCR System equipped with 96-well optical reaction plates. Each $20\,\mu$l reaction contained $1 \times$ SYBR Green PCR Master Mix (Applied Biosystems), 100 ng cDNA and 250 nM of each specific primer. The primers used for SYBR Green RT-qPCR were: CD40, 5′-CTG TTT GCC ATC CTC TTG GT-3′ (sense) and 5′-CGA CTC TCT TTG CCA TCC TC-3′ (antisense); CD40L, 5′-ATT GGG TCA GCA CTT TTT GC-3′ (sense) and 5′-TCA CAA AGC CTT CAA ACT GG-3′ (antisense); and GAPDH, 5′-GAG TCA ACG GAT TTG GTC GT-3′ (sense) and 5′-GAC AAG CTT CCC GTT CTC AG-3′ (antisense). The specificity of each assay was validated by dissociation curve analysis and agarose gel electrophoresis of PCR products. Assay performance was validated by evaluating amplification efficiencies by means of calibration curves, and ensuring that the plot of log input amount *versus* ΔCq has a slope $< |0.1|$. Alternatively, TaqMan gene expression assays were used for AIF, EndoG and GAPDH (Hs00377585_m1, Hs01035290_m1 and Hs02758991_g1, respectively; Applied Biosystems). Each $20\,\mu$l TaqMan reaction contained $1 \times$ TaqMan Gene Expression Master Mix (Applied Biosystems), 100 ng cDNA and $1 \times$ TaqMan gene expression assay (containing primers and probe). The PCR parameters for SYBR Green and TaqMan RT-qPCR were 50 °C for 2 min, 95 °C for 10 min, and 40 cycles of 95 °C for 15 s and 60 °C for 1 min. All RT-qPCR results represent the mean of at least three separate experiments and each sample was assayed in triplicate. Relative quantification of mRNA levels was performed by the comparative Cq method with GAPDH as the reference gene and using the formula $2^{-\Delta\Delta Cq}$.

MTT and Trypan blue exclusion assays. For the MTT assay, cells were seeded at a density of 2×10^4 cells/well in 48-well plates and treated as described. MTT was added to a final concentration of 0.5 mg/ml, the cells were incubated for 4 h and the medium was removed. DMSO was added to each well and absorbances were measured at 490 nm using a microplate reader. For the Trypan blue exclusion assay, cells were seeded at a density of 5×10^4 cells/well in 12-well plates and treated as described. Viable cell numbers were counted by Trypan blue dye

exclusion using a hemocytometer. Results are expressed as a percentage relative to vehicle-treated control.

Statistical analysis. Results are presented as the mean $\pm$ S.E.M. of at least three separate experiments, and were analyzed by *t*-test or one-way ANOVA followed by Student-Newman-Keuls multiple comparison test using PRISM software (GraphPad Software, Inc., San Diego, CA, USA). Significant differences were defined as $P < 0.05$.

Conflict of Interest

The authors declare no conflict interest.

1. Crispens MA, Bodurka D, Deavers M, Lu K, Silva EG, Gershenson DM. Response and survival in patients with progressive or recurrent serous ovarian tumors of low malignant potential. *Obstet Gynecol* 2002; **99**: 3–10.
2. Landen Jr CN, Birrer MJ, Sood AK. Early events in the pathogenesis of epithelial ovarian cancer. *J Clin Oncol* 2008; **26**: 995–1005.
3. Silva EG, Gershenson DM, Malpica A, Deavers M. The recurrence and the overall survival rates of ovarian serous borderline neoplasms with noninvasive implants is time dependent. *Am J Surg Pathol* 2006; **30**: 1367–1371.
4. Shih Ie M, Kurman RJ. Ovarian tumorigenesis: a proposed model based on morphological and molecular genetic analysis. *Am J Pathol* 2004; **164**: 1511–1518.
5. Singer G, Kurman RJ, Chang HW, Cho SK, Shih Ie M. Diverse tumorigenic pathways in ovarian serous carcinoma. *Am J Pathol* 2002; **160**: 1223–1228.
6. Cheng JC, Auersperg N, Leung PC. EGF-induced EMT and invasiveness in serous borderline ovarian tumor cells: a possible step in the transition to low-grade serous carcinoma cells? *PLoS One* 2012; **7**: e34071.
7. Cheng JC, Auersperg N, Leung PC. TGF-beta induces serous borderline ovarian tumor cell invasion by activating EMT but triggers apoptosis in low-grade serous ovarian carcinoma cells. *PloS one* 2012; **7**: e42436.
8. Cheng JC, Auersperg N, Leung PC. Inhibition of p53 induces invasion of serous borderline ovarian tumor cells by accentuating PI3K/Akt-mediated suppression of E-cadherin. *Oncogene* 2011; **30**: 1020–1031.
9. Cheng JC, Auersperg N, Leung PC. Inhibition of p53 represses E-cadherin expression by increasing DNA methyltransferase-1 and promoter methylation in serous borderline ovarian tumor cells. *Oncogene* 2011; **30**: 3930–3942.
10. Gershenson DM, Sun CC, Bodurka D, Coleman RL, Lu KH, Sood AK *et al*. Recurrent low-grade serous ovarian carcinoma is relatively chemoresistant. *Gynecol Oncol* 2009; **114**: 48–52.
11. van Kooten C, Banchereau J. CD40-CD40 ligand. *J Leukoc Biol* 2000; **67**: 2–17.
12. Grewal IS, Flavell RA. CD40 and CD154 in cell-mediated immunity. *Annu Rev Immunol* 1998; **16**: 111–135.
13. Fonsatti E, Maio M, Altomonte M, Hersey P. Biology and clinical applications of CD40 in cancer treatment. *Semin Oncol* 2010; **37**: 517–523.
14. Gomes EM, Rodrigues MS, Phadke AP, Butcher LD, Starling C, Chen S *et al*. Antitumor activity of an oncolytic adenoviral-CD40 ligand (CD154) transgene construct in human breast cancer cells. *Clin Cancer Res* 2009; **15**: 1317–1325.
15. Wang X, Chen B, Xu W, Liu S, Zhao W, Wu J. Combined effects of klotho and soluble CD40 ligand on A549 lung cancer cells. *Oncol Rep* 2011; **25**: 1465–1472.
16. Fiumara P, Younes A. CD40 ligand (CD154) and tumour necrosis factor-related apoptosis inducing ligand (Apo-2L) in haematological malignancies. *Br J Haematol* 2001; **113**: 265–274.
17. Planken EV, Dijkstra NH, Willemze R, Kluin-Nelemans JC. Proliferation of B cell malignancies in all stages of differentiation upon stimulation in the 'CD40 system'. *Leukemia* 1996; **10**: 488–493.
18. Baxendale AJ, Dawson CW, Stewart SE, Mudaliar V, Reynolds G, Gordon J *et al*. Constitutive activation of the CD40 pathway promotes cell transformation and neoplastic growth. *Oncogene* 2005; **24**: 7913–7923.
19. Homig-Holzel C, Hojer C, Rastelli J, Casola S, Strobl LJ, Muller W *et al*. Constitutive CD40 signaling in B cells selectively activates the noncanonical NF-kappaB pathway and promotes lymphomagenesis. *J Exp Med* 2008; **205**: 1317–1329.
20. Zhou Y, He J, Gou LT, Mu B, Liao WC, Ma C *et al*. Expression of CD40 and growth-inhibitory activity of CD40 agonist in ovarian carcinoma cells. *Cancer Immunol Immunother* 2012; **61**: 1735–1743.
21. Gallagher NJ, Eliopoulos AG, Agathangelo A, Oates J, Crocker J, Young LS. CD40 activation in epithelial ovarian carcinoma cells modulates growth, apoptosis, and cytokine secretion. *Mol Pathol* 2002; **55**: 110–120.

22. Hakkarainen T, Hemminki A, Pereboev AV, Barker SD, Asiedu CK, Strong TV *et al*. CD40 is expressed on ovarian cancer cells and can be utilized for targeting adenoviruses. *Clin Cancer Res* 2003; **9**: 619–624.

23. Toutirais O, Gervais A, Cabillic F, Le Gallo M, Coudrais A, Leveque J *et al*. Effects of CD40 binding on ovarian carcinoma cell growth and cytokine production in vitro. *Clin Exp Immunol* 2007; **149**: 372–377.

24. Melichar B, Patenia R, Gallardo S, Melicharova K, Hu W, Freedman RS. Expression of CD40 and growth-inhibitory activity of CD40 ligand in ovarian cancer cell lines. *Gynecol Oncol* 2007; **104**: 707–713.

25. Ghamande S, Hylander BL, Oflazoglu E, Lele S, Fanslow W, Repasky EA. Recombinant CD40 ligand therapy has significant antitumor effects on CD40-positive ovarian tumor xenografts grown in SCID mice and demonstrates an augmented effect with cisplatin. *Cancer Res* 2001; **61**: 7556–7562.

26. Shih Ie M, Chen L, Wang CC, Gu J, Davidson B, Cope L *et al*. Distinct DNA methylation profiles in ovarian serous neoplasms and their implications in ovarian carcinogenesis. *Am J Obstet Gynecol* 2010; **203**: 584 e581–522.

27. Anglesio MS, Wiegand KC, Melnyk N, Chow C, Salamanca C, Prentice LM *et al*. Type-specific cell line models for type-specific ovarian cancer research. *PLoS One* 2013; **8**: e72162.

28. Luthi AU, Martin SJ. The CASBAH: a searchable database of caspase substrates. *Cell Death Differ* 2007; **14**: 641–650.

29. Timmer JC, Salvesen GS. Caspase substrates. *Cell Death Differ* 2007; **14**: 66–72.

30. Mayer B, Oberbauer R. Mitochondrial regulation of apoptosis. *News in Physiological Sciences* 2003; **18**: 89–94.

31. Zamzami N, Kroemer G. The mitochondrion in apoptosis: how Pandora's box opens. *Nat Rev Mol Cell Biol* 2001; **2**: 67–71.

32. Susin SA, Lorenzo HK, Zamzami N, Marzo I, Snow BE, Brothers GM *et al*. Molecular characterization of mitochondrial apoptosis-inducing factor. *Nature* 1999; **397**: 441–446.

33. Li LY, Luo X, Wang X. Endonuclease G is an apoptotic DNase when released from mitochondria. *Nature* 2001; **412**: 95–99.

34. Vandenabeele P, Galluzzi L, Vanden Berghe T, Kroemer G. Molecular mechanisms of necroptosis: an ordered cellular explosion. *Nat Rev Mol Cell Biol* 2010; **11**: 700–714.

35. de Almagro MC, Vucic D. Necroptosis: Pathway diversity and characteristics. *Semin Cell Dev Biol* 2015; **39**: 56–62.

36. Degterev A, Maki JL, Yuan J. Activity and specificity of necrostatin-1, small-molecule inhibitor of RIP1 kinase. *Cell Death Differ* 2013; **20**: 366.

37. Takahashi N, Duprez L, Grootjans S, Cauwels A, Nerinckx W, DuHadaway JB *et al*. Necrostatin-1 analogues: critical issues on the specificity, activity and in vivo use in experimental disease models. *Cell Death Dis* 2012; **3**: e437.

38. Sun L, Wang H, Wang Z, He S, Chen S, Liao D *et al*. Mixed lineage kinase domain-like protein mediates necrosis signaling downstream of RIP3 kinase. *Cell* 2012; **148**: 213–227.

39. Eliopoulos AG, Davies C, Knox PG, Gallagher NJ, Afford SC, Adams DH *et al*. CD40 induces apoptosis in carcinoma cells through activation of cytotoxic ligands of the tumor necrosis factor superfamily. *Mol Cell Biol* 2000; **20**: 5503–5515.

40. Tong AW, Papayoti MH, Netto G, Armstrong DT, Ordonez G, Lawson JM *et al*. Growth-inhibitory effects of CD40 ligand (CD154) and its endogenous expression in human breast cancer. *Clin Cancer Res* 2001; **7**: 691–703.

41. Hess S, Engelmann H. A novel function of CD40: induction of cell death in transformed cells. *J Exp Med* 1996; **183**: 159–167.

42. von Leoprechting A, van der Bruggen P, Pahl HL, Aruffo A, Simon JC. Stimulation of CD40 on immunogenic human malignant melanomas augments their cytotoxic T lymphocyte-mediated lysis and induces apoptosis. *Cancer Res* 1999; **59**: 1287–1294.

43. Hirano A, Longo DL, Taub DD, Ferris DK, Young LS, Eliopoulos AG *et al*. Inhibition of human breast carcinoma growth by a soluble recombinant human CD40 ligand. *Blood* 1999; **93**: 2999–3007.

44. Hassan SB, Sorensen JF, Olsen BN, Pedersen AE. Anti-CD40-mediated cancer immunotherapy: an update of recent and ongoing clinical trials. *Immunopharmacol Immunotoxicol* 2014; **36**: 96–104.

45. Lanzavecchia A. Immunology. Licence to kill. *Nature* 1998; **393**: 413–414.

46. Todryk SM, Tutt AL, Green MH, Smallwood JA, Halanek N, Dalgleish AG *et al*. CD40 ligation for immunotherapy of solid tumours. *J Immunol Methods* 2001; **248**: 139–147.

47. Vonderheide RH, Bajor DL, Winograd R, Evans RA, Bayne LJ, Beatty GL. CD40 immunotherapy for pancreatic cancer. *Cancer Immunol Immunother* 2013; **62**: 949–954.

48. Lum HD, Buhtoiarov IN, Schmidt BE, Berke G, Paulnock DM, Sondel PM *et al*. In vivo CD40 ligation can induce T-cell-independent antitumor effects that involve macrophages. *J Leukoc Biol* 2006; **79**: 1181–1192.

49. Beatty GL, Chiorean EG, Fishman MP, Saboury B, Teitelbaum UR, Sun W *et al*. CD40 agonists alter tumor stroma and show efficacy against pancreatic carcinoma in mice and humans. *Science* 2011; **331**: 1612–1616.

50. Coughlin CM, Vance BA, Grupp SA, Vonderheide RH. RNA-transfected CD40-activated B cells induce functional T-cell responses against viral and tumor antigen targets: implications for pediatric immunotherapy. *Blood* 2004; **103**: 2046–2054.

51. Turner JG, Rakhmilevich AL, Burdelya L, Neal Z, Imboden M, Sondel PM *et al*. Anti-CD40 antibody induces antitumor and antimetastatic effects: the role of NK cells. *J Immunol* 2001; **166**: 89–94.

52. Rakhmilevich AL, Alderson KL, Sondel PM. T-cell-independent antitumor effects of CD40 ligation. *Int Rev Immunol* 2012; **31**: 267–278.

53. Galluzzi L, Vitale I, Abrams JM, Alnemri ES, Baehrecke EH, Blagosklonny MV *et al*. Molecular definitions of cell death subroutines: recommendations of the Nomenclature Committee on Cell Death 2012. *Cell Death Differ* 2012; **19**: 107–120.

54. Kroemer G, Galluzzi L, Vandenabeele P, Abrams J, Alnemri ES, Baehrecke EH *et al*. Classification of cell death: recommendations of the Nomenclature Committee on Cell Death 2009. *Cell Death Differ* 2009; **16**: 3–11.

55. Elmore S. Apoptosis: a review of programmed cell death. *Toxicol Pathol* 2007; **35**: 495–516.

56. Yi CH, Yuan J. The Jekyll and Hyde functions of caspases. *Dev Cell* 2009; **16**: 21–34.

57. Connolly PF, Jager R, Fearnhead HO. New roles for old enzymes: killer caspases as the engine of cell behavior changes. *Front Physiol* 2014; **5**: 149.

58. Zermati Y, Garrido C, Amsellem S, Fishelson S, Bouscary D, Valensi F *et al*. Caspase activation is required for terminal erythroid differentiation. *J Exp Med* 2001; **193**: 247–254.

59. Carlile GW, Smith DH, Wiedmann M. Caspase-3 has a nonapoptotic function in erythroid maturation. *Blood* 2004; **103**: 4310–4316.

60. Woo M, Hakem R, Furlonger C, Hakem A, Duncan GS, Sasaki T *et al*. Caspase-3 regulates cell cycle in B cells: a consequence of substrate specificity. *Nat Immunol* 2003; **4**: 1016–1022.

61. Janzen V, Fleming HE, Riedt T, Karlsson G, Riese MJ, Lo Celso C *et al*. Hematopoietic stem cell responsiveness to exogenous signals is limited by caspase-3. *Cell Stem Cell* 2008; **2**: 584–594.

62. Fujita J, Crane AM, Souza MK, Dejosez M, Kyba M, Flavell RA *et al*. Caspase activity mediates the differentiation of embryonic stem cells. *Cell Stem Cell* 2008; **2**: 595–601.

63. Tait SW, Green DR. Caspase-independent cell death: leaving the set without the final cut. *Oncogene* 2008; **27**: 6452–6461.

64. Cho YS, Challa S, Moquin D, Genga R, Ray TD, Guildford M *et al*. Phosphorylation-driven assembly of the RIP1-RIP3 complex regulates programmed necrosis and virus-induced inflammation. *Cell* 2009; **137**: 1112–1123.

65. He S, Wang L, Miao L, Wang T, Du F, Zhao L *et al*. Receptor interacting protein kinase-3 determines cellular necrotic response to TNF-alpha. *Cell* 2009; **137**: 1100–1111.

66. Zhang DW, Shao J, Lin J, Zhang N, Lu BJ, Lin SC *et al*. RIP3, an energy metabolism regulator that switches TNF-induced cell death from apoptosis to necrosis. *Science* 2009; **325**: 332–336.

67. Festjens N, Vanden Berghe T, Cornelis S, Vandenabeele P. RIP1, a kinase on the crossroads of a cell's decision to live or die. *Cell Death Differ* 2007; **14**: 400–410.

68. Abhari BA, Cristofanon S, Kappler R, von Schweinitz D, Humphreys R, Fulda S. RIP1 is required for IAP inhibitor-mediated sensitization for TRAIL-induced apoptosis via a RIP1/FADD/caspase-8 cell death complex. *Oncogene* 2013; **32**: 3263–3273.

69. Lin Y, Devin A, Rodriguez Y, Liu ZG. Cleavage of the death domain kinase RIP by caspase-8 prompts TNF-induced apoptosis. *Genes Dev* 1999; **13**: 2514–2526.

70. Knox PG, Davies CC, Ioannou M, Eliopoulos AG. The death domain kinase RIP1 links the immunoregulatory CD40 receptor to apoptotic signaling in carcinomas. *J Cell Biol* 2011; **192**: 391–399.

71. Kearney CJ, Cullen SP, Clancy D, Martin SJ. RIPK1 can function as an inhibitor rather than an initiator of RIPK3-dependent necroptosis. *FEBS J* 2014; **281**: 4921–4934.

72. Weiss WA, Taylor SS, Shokat KM. Recognizing and exploiting differences between RNAi and small-molecule inhibitors. *Nat Chem Biol* 2007; **3**: 739–744.

73. Woo MM, Salamanca CM, Symowicz J, Stack MS, Miller DM, Leung PC *et al*. SV40 early genes induce neoplastic properties in serous borderline ovarian tumor cells. *Gynecol Oncol* 2008; **111**: 125–131.

74. Woo MM, Salamanca CM, Miller M, Symowicz J, Leung PC, Oliveira C *et al*. Serous borderline ovarian tumors in long-term culture: phenotypic and genotypic distinction from invasive ovarian carcinomas. *Int J Gynecol Cancer* 2008; **18**: 1234–1247.

75. Pohl G, Ho CL, Kurman RJ, Bristow R, Wang TL, Shih Ie M. Inactivation of the mitogen-activated protein kinase pathway as a potential target-based therapy in ovarian serous tumors with KRAS or BRAF mutations. *Cancer Res* 2005; **65**: 1994–2000.

Supplementary Information accompanies this paper on Cell Death and Disease website (http://www.nature.com/cddis)